CHIN. PHYS. LETT. Vol. 37, No. 4 (2020) 047201

Negative Magnetoresistance in Antiferromagnetic Topological Insulator $EuSn_2As_2$*

Huan-Cheng Chen(陈奂丞)[1], Zhe-Feng Lou(娄哲丰)[1], Yu-Xing Zhou(周宇星)[1], Qin Chen(陈琴)[1], Bin-Jie Xu(许彬杰)[1], Shui-Jin Chen(陈水金)[1], Jian-Hua Du(杜建华)[2], Jin-Hu Yang(杨金虎)[3], Hang-Dong Wang(王杭栋)[3], Ming-Hu Fang(方明虎)[1,4]**

[1]*Department of Physics, Zhejiang University, Hangzhou 310027*
[2]*Department of Applied Physics, China Jiliang University, Hangzhou 310018*
[3]*Department of Physics, Hangzhou Normal University, Hangzhou 310036*
[4]*Collaborative Innovation Center of Advanced Microstructures, Nanjing University, Nanjing 210093*

(Received 12 February 2020)

The measurements of magnetization, longitudinal and Hall resistivities are carried out on the intrinsic antiferromagnetic (AFM) topological insulator $EuSn_2As_2$. It is confirmed that our $EuSn_2As_2$ crystal is a heavily hole doping A-type AFM metal with the Néel temperature $T_N = 24$ K, with a metamagnetic transition from an AFM to a ferromagnetic (FM) phase occurring at a certain critical magnetic field for the different field orientations. Meanwhile, we also find that the carrier concentration does not change with the evolution of magnetic order, indicating that the weak interaction between the localized magnetic moments from Eu^{2+} $4f^7$ orbits and the electronic states near the Fermi level. Although the quantum anomalous Hall effect (AHE) is not observed in our crystals, it is found that a relatively large negative magnetoresistance (−13%) emerges in the AFM phase, and exhibits an exponential dependence upon magnetic field, whose microscopic origin is waiting to be clarified in future research.

PACS: 72.15.−v, 75.47.−m, 75.50.Ee DOI: 10.1088/0256-307X/37/4/047201

In the time-reversal-invariant Z_2 topological insulator (TI), the existence of magnetism can produce many exotic topological quantum phenomena, such as the quantum anomalous Hall effect (AHE),[1−6] axion insulator states[7−10] and chiral Majorana fermions.[11] To seek for magnetic TI attracts much attention in the condensed matter physics community in the past ten years. First, the quantum AHE was realized in magnetically doped $(Bi, Sb)_2Te_3$ thin film,[2,3] in which the existence of unavoidable disorder results in the emergence of AHE at very low temperature (<100 mK). Then, a lot of promising candidates for magnetic Weyl semimetals were proposed, including $Y_2Ir_2O_7$,[12] $HgCr_2Se_4$,[13] and some magnetic Heusler compounds.[14−18] The quantum AHE is expected to appear in thin films of magnetic Weyl semimetals. In the last year, theory predicts several intrinsic antiferromagnetic (AFM) TIs, such as $MnBi_2Te_4$[8,19−22] and $EuIn_2As_2$,[23] which were soon confirmed by the experiments,[24,25] and a quantized Hall plateau at $\hbar/e^2$ was discovered in the few-layer $MnBi_2Te_4$ flake. Recently, by combining first-principles calculations and angle-resolved photoemission spectroscopy (ARPES) experiments, Li *et al.*[26] revealed that $EuSn_2As_2$ is an AFM TI with Dirac surface states, but with no observable gap inside, which is different from the large gap of tens of meV in another AFM TI family, $MnBi_{2n}Te_{3n+1}$ ($n = 1$ and 2).[8,10,21] They also found[26] that the Dirac surface states have almost no change when long-range AFM order develops, which is attributed to weak coupling between the local magnetic moments and the topological electronic states. On the other hand, $EuSn_2As_2$[27] is a layered magnetic Zintl–Klemm compound with a van der Waals bonding between neighboring layers, in which Eu^{2+} $4f^7$ spins magnetically order at 24 K and are coupled ferromagnetically within layer, and antiferromagnetically between adjacent layers, providing a platform to study the layer-dependent magnetic properties.

In this Letter, on the basis of successfully growing $EuSn_2As_2$ single crystals, we measured the magnetization, longitudinal and Hall resistivity with various magnetic field orientations relative to its c axis. It was verified that $EuSn_2As_2$ is an A-type antiferromagnet with Néel temperature $T_N = 24$ K, and exhibits a metamagnetism from an AFM phase at lower fields changing to an FM phase at higher fields. Interestingly, it was found that a relatively large negative magnetoresistance (MR) emerges in the AFM phase, and depends exponentially upon magnetic field $\mu_0 H$ ($\propto M$).

*Supported by the National Key Research and Development Program of China under Grant No. 2016YFA0300402, the National Basic Research Program of China under Grant No. 2015CB921004, the National Natural Science Foundation of China under Grant Nos. 11974095 and 11374261, the Zhejiang Natural Science Foundation (No. LY16A040012), and the Fundamental Research Funds for the Central Universities.

**Corresponding author. Email: mhfang@zju.edu.cn

© 2020 Chinese Physical Society and IOP Publishing Ltd

Single crystals of $EuSn_2As_2$ were grown by a self-flux method. High-purity Eu, Sn and As powder were mixed in the mole ratio 1 : 21 : 2, then sealed in an evacuated silica tube. The quartz tube was placed in a furnace, and heated to 850℃ and held for 24 hrs, then cooled slowly to room temperature for one week. The shiny platelet-like $EuSn_2As_2$ single crystals were obtained with a mechanical exfoliation method. A single crystal with dimension of $1.0 \times 1.5 \times 0.25\,\text{mm}^3$ [see the inset of Fig. 1(c)] was selected for the transport and magnetic properties measurements. The single crystal x-ray diffraction (XRD) was carried out using a PANalytical diffractometer, as shown in Fig. 1(c), to determine the c-axis length as $c = 26.463(3)$ Å, in agreement with the result reported in Ref. [27]. The longitudinal and Hall resistivity measurements were performed on a Quantum Design physical properties measurement system (PPMS-9T) with a standard four-probe method. The magnetization measurements were carried out on a Quantum Design magnetic properties measurement system (MPMS-7T).

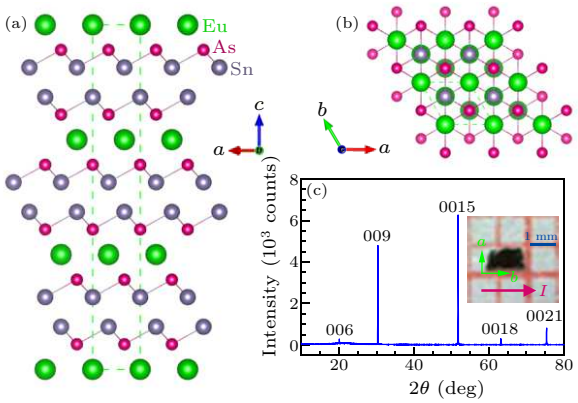

Fig. 1. [(a), (b)] Crystal structure of $EuSn_2As_2$. (c) Single crystal XRD pattern and the photograph of $EuSn_2As_2$ crystal.

First, we check the magnetic properties of $EuSn_2As_2$ crystal. Figure 2(a) shows the temperature dependence of magnetic susceptibility, $\chi(T)$, measured at applied magnetic field of 0.5 T with both perpendicular and parallel to c-axis orientations and with field-cooling process, the magnetic susceptibility increases with decreasing temperature, and exhibits a kink at 24 K for both magnetic field orientations, indicating that an AFM transition occurs with the Nèel temperature $T_N = 24$ K. Compared with the susceptibilities measured at $H \| c$ axis, the larger in-plane susceptibilities below T_N implies that the spins of Eu^{2+} $4f^7$ electrons are coupled ferromagnetically within ab planes, and antiferromagntically between adjacent layers, which is consistent with that reported preciously for both $EuSn_2As_2$[27] and $EuSn_2P_2$,[28] called the A-type AFM. The susceptibility measured with both field orientations in the paramagnetic (PM) phase above T_N can be well described by the Curie–Weiss law $\chi = \frac{C}{T-\theta}$, as shown in the inset of Fig. 2(a). The obtained effective moment μ_{eff} (= 7.84 and $7.99\,\mu_B/Eu^{2+}$) value for both H (perpendicular and parallel to the c-axis, respectively) orientations is very close to the theoretical value ($7.94\,\mu_B/Eu^{2+}$), and the Curie–Weiss temperature θ (= 24.92 and 23.17 K) is close to the value of T_N, indicating that the Eu^{2+} $4f^7$ electrons are localized. This is in good agreement with the result of the band calculation,[26] which revealed that the localized Eu^{2+} $4f^7$ states are localized at approximately 1.7 eV below Fermi level E_F and have negligible coupling with the other bands near E_F. The isothermal magnetization as a function of magnetic field, $M(H)$, measured at 2 K with both field orientations is presented in Fig. 2(b). Magnetization increases linearly with increasing magnetic field at first, then saturates to $6.75\mu_B$ and $6.90\mu_B$ values, at a critical field $\mu_0 H_c$ of 3.5 T and 4.75 T, respectively, for $H \perp$ and $\| c$-axis, indicating that a metamagnetic transition from AFM to FM occurs at different H_c for both orientations, implying the anisotropy of magnetic coupling.

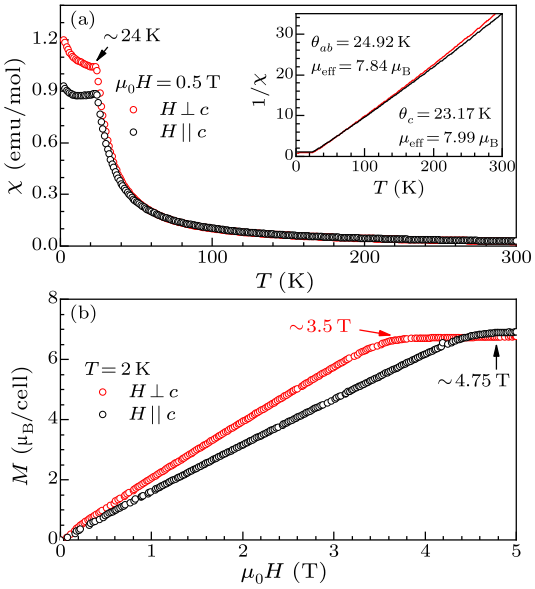

Fig. 2. (a) Temperature dependence of magnetic susceptibility, $\chi(T)$, measured at magnetic field 0.5 T applied perpendicular and parallel to the c axis. Inset: the temperature dependence of inverse susceptibility for both orientations. (b) Isothermal magnetization as a function of magnetic field $\mu_0 H$, measured at 2 K with both perpendicular and parallel to the c-axis magnetic field orientations.

Next, we discuss the transport properties of $EuSn_2As_2$ crystal. Figure 3(a) shows the temperature dependence of longitudinal resistivity, $\rho(T)$, measured at zero-field. The resistivity decreases first with decreasing temperature, reaches a minimum at about 40 K, then increases a little before dropping again below $T_N \sim 24$ K. In the PM state, the minimum exhibiting in $\rho(T)$ is usually attributed to the Kondo scattering of spin disorder.[29,30] As the long-range AFM

order occurs below T_N, the resistivity decreases due to the reduction of the Kondo scattering. Considering that $EuSn_2As_2$ transforms from a strong TI ($Z_2 = 1$) in the PM state to an axion insulator ($Z_4 = 2$) in the AFM state,[26] we measured the magnetoresistance (MR) in both states. Figure 3(b) presents the MR measured at different temperatures as a function of magnetic field $\mu_0 H$ applied along the c axis, here MR is defined as

$$\mathrm{MR} = \frac{\rho(\mathrm{H}) - \rho(0)}{\rho(0)} \times 100\%, \qquad (1)$$

where $\rho(H)$ and $\rho(0)$ are the resistivities measured at magnetic field $\mu_0 H$ and zero field, respectively.

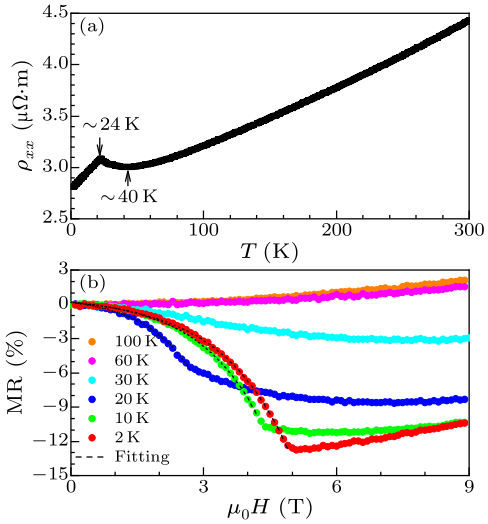

Fig. 3. (a) Temperature dependence of longitudinal resistivity, $\rho(T)$, measured at zero field. (b) Magnetoresistance as a function of magnetic field, $\mu_0 H$, applied along the c axis, measured at various temperatures. The black dotted lines are the fit to the experimental data in AFM phase measured at 2 K, 10 K and 20 K, respectively, using the exponential form, as mentioned in the text.

It can be seen that the MRs in both PM and AFM phases exhibit a different behavior. In the PM phase (T = 60, 100 K, above T_N), the MR increases a little (~2%) with increasing $\mu_0 H$ up to 9 T, exhibiting a small positive MR enhanced by temperature, which is consistent with the theoretical calculation[31] for the magnetic metals. When the temperature decreases to 30 K (just above $T_N \sim 24$ K), the MR becomes a negative, and decreases with increasing magnetic field, then saturates to about −3% up to 9 T. As the temperature decreases further much lower than T_N, e.g., at 2 K, with increasing magnetic field, the MR decreases gradually at first, reaches a minimum of −13% at $\mu_0 H = 4.75$ T, then increases linearly to −9%, which seems to be related to the metamagnetic transition mentioned above. In the FM phase, a small positive MR (4%) occurs, which is also consistent with the theory prediction.[31] Interestingly, in the AFM phase ($\mu_0 H < \mu_0 H_c = 4.75$ T, at 2 K), the MR depends exponentially upon $\mu_0 H$ ($\sim M$), as shown in Fig. 3(b), i.e., MR = $-\alpha \exp(\beta H)$. The fit to MR data measured at 2 K, 10 K, and 20 K yields the parameters $\alpha = (0.53 \pm 0.02\%)$, nearly independent of temperature; $\beta = (0.65 \pm 0.01)$, (0.71 ± 0.04), and (0.92 ± 0.04), respectively, which enhances with increasing temperature. The negative MR is as large as 13% at 2 K, much lower than T_N, implying that this MR does not clearly originate from a critical-point effect. Theory predicts[31] that the MR in an AFM metal should be either (a) positive varying as H^2 ($\sim M^2$) if the magnetic field is applied along the easy axis or (b) negligible if the magnetic field is perpendicular to the easy axis. In contrast the these expectations, the MR in the AFM phase of $EuSn_2As_2$ is negative, and certainly not small, and exhibits a exponential dependence upon the magnetic field $\mu_0 H$ ($\sim M$), similar to that observed[32] in the FM phase for the colossal magnetoresistance (CMR) compounds (La,Ca)MnO_3. This behavior of MR in the manganites was explained as the result of hopping of magnetic polarons[33] composed of an electron which ferromagnetically polarizes the surrounding ionic magnetic moments due to the strong coupling between structure and magnetism. However, in $EuSn_2As_2$, it is impossible to explain the MR behavior in the AFM phase using this scenario due to the weak hybridization between Eu^{2+} $4f^7$ orbits providing the localized magnetic moments and the electronic states near E_F contributing conduction carriers. The microscopic mechanism of the relatively large negative MR emerging in this intrinsic AFM TI is worthy to investigate in the future.

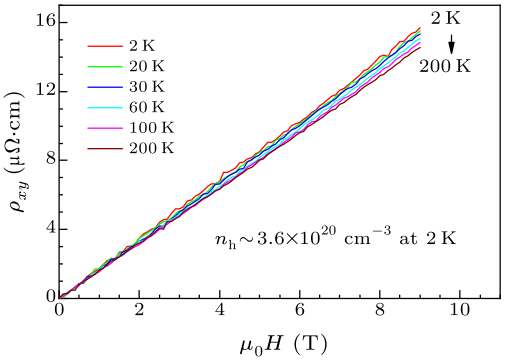

Fig. 4. Field dependence of Hall resistivity ρ_{xy} measured at various temperatures with applied magnetic field along the c axis.

Finally, to get the information about the charge carriers, we measured the Hall resistivity of $EuSn_2As_2$ at different temperatures. Figure 4 shows the Hall resistivity ρ_{xy} as a function of magnetic field $\mu_0 H$, measured in the temperature range of 2–200 K with applied magnetic field along the c axis. The linear $\rho_{xy}(H)$ with a positive slope indicates that the hole carriers are dominated in our crystals. It can be seen

that the slope of $\rho_{xy}(H)$ in all the measurement temperature range of 2–200 K is almost the same, implying no remarkable change in the carrier concentration $n_{\rm h}$ with temperature, such as the obtained $n_{\rm h} = 3.60 \times 10^{20}\,{\rm cm}^{-3}$ at 2 K, $n_{\rm h} = 3.79 \times 10^{20}\,{\rm cm}^{-3}$ at 100 K, $n_{\rm h} = 3.87 \times 10^{20}\,{\rm cm}^{-3}$ at 200 K, which are relatively larger than that in $EuSn_2P_2$.[28] It should be noted that the evolution of magnetic order (from PM to AFM with decreasing temperature, from AFM to FM with increasing magnetic field) does not change visibly $n_{\rm h}$, and AHE expected to occur in the intrinsic magnetic TI has not been observed in our $EuSn_2As_2$ crystal, even in the FM phase. This may be due to weak hybridization between the localized magnetic moments from $Eu^{2+}\,4f^7$ orbital and the topological electronic states.

In summary, we have successfully grown $EuSn_2As_2$ single crystals using a self-flux method, which is recently confirmed to be an intrinsic AFM TI. Also, we have measured its magnetization, longitudinal and Hall resistivity. It is confirmed that $EuSn_2As_2$ crystal is a heavily hole doping A-type AFM metal, with a metamagnetic transition from an AFM to an FM phase. We find that the carrier concentration does not change with the evolution of magnetic order. Although the AHE is not observed in our crystals, it is found that a relatively large negative magnetoresistance (−13%) emerges in the AFM phase, and exhibits an exponential dependence upon the magnetic field.

References

[1] Mong R S K, Essin A M and Moore J E 2010 *Phys. Rev. B* **81** 245209
[2] Yu R, Zhang W, Zhang H J, Zhang S C, Dai X and Fang Z 2010 *Science* **329** 61
[3] Chang C Z, Zhang J S, Feng X, Shen J, Zhang Z C, Guo M H, Li K, Ou Y B, Wei P, Wang L L, Ji Z Q, Feng Y, Ji S H, Chen X, Jia J F, Dai X, Fang Z, Zhang S C, He K, Wang Y Y, Lu L, Ma X C and Xue Q K 2013 *Science* **340** 167
[4] Checkelsky J G, Yoshimi R, Tsukazaki A, Takahashi K S, Kozuka Y, Falson J, Kawasaki M and Tokura Y 2014 *Nat. Phys.* **10** 731
[5] Kou X F, Guo S T, Fan Y B, Pan L, Lang M R, Jiang Y, Shao Q M, Nie T X, Tang J S, Wang Y, He L, Lee T K, Lee W L and Wang K L 2014 *Phys. Rev. Lett.* **113** 137201
[6] Chang C Z, Zhao W W, Kim D Y, Zhang H J, Assaf B A, Heiman D, Zhang S C, Liu C X, Chan M H W and Moodera J S 2015 *Nat. Mater.* **14** 473
[7] Mogi M, Kawamura M, Yoshimi R, Tsukazaki A, Kozuka Y, Shirakawa N, Takahashi K S, Kawasaki M and Tokura Y 2017 *Nat. Mater.* **16** 516
[8] Zhang D Q, Shi M J, Zhu T S, Xing D Y, Zhang H J and Wang J 2019 *Phys. Rev. Lett.* **122** 206401
[9] Wang J, Lian B, Qi X L and Zhang S C 2015 *Phys. Rev. B* **92** 081107
[10] Gong Y, Guo J W, Li J H, Zhu K J, Liao M H, Liu X Z, Zhang J H, Gu L, Tang L, Feng X, Zhang D, Li W, Song C L, Wang L L, Yu P, Chen X, Wang Y X, Yao H, Duan W H, Xu Y, Zhang S C, Ma X C, Xue Q K and He K 2019 *Chin. Phys. Lett.* **36** 076801
[11] Qi X L, Hughes T L and Zhang S C 2010 *Phys. Rev. B* **82** 184516
[12] Wan X G, Turner A M, Vishwanath A and Savrasov S Y 2011 *Phys. Rev. B* **83** 205101
[13] Xu G, Weng H M, Wang Z J, Dai X, Fang Z 2011 *Phys. Rev. Lett.* **107** 186806
[14] Kübler J and Felser C 2016 *Europhys. Lett.* **114** 47005
[15] Wang Z J, Vergniory M G, Kushwaha S, Hirschberger M, Chulkov E V, Ernst A, Ong N P, Cava R J and Bernevig B A 2016 *Phys. Rev. Lett.* **117** 236401
[16] Chang G Q, Xu S Y, Zheng H, Singh B, Hsu C H, Bian G, Alidoust N, Belopolski I, Sanchez D S, Zhang S T, Lin H and Hasan M Z 2016 *Sci. Rep.* **6** 38839
[17] Zhang J H, Zhang S, Chen Z H, Lv M, Zhao H C, Yang Y F, Chen G F and Sun P J 2018 *Chin. Phys. B* **27** 097103
[18] Wang Q, Du Q H, Petrovic C and Lei H C 2020 *Chin. Phys. Lett.* **37** 027502
[19] Li J H, Wang C, Zhang Z T, Gu B L, Duan W H and Xu Y 2019 *Phys. Rev. B* **100** 121103
[20] Otrokov M M, Rusinov I P, Blanco-Rey M, Hoffmann M, Vyazovskaya A Y, Eremeev S V, Ernst A, Echenique P M, Arnau A and Chulkov E V 2019 *Phys. Rev. Lett.* **122** 107202
[21] Li J H, Li Y, Du S Q, Wang Z, Gu B L, Zhang S C, He K, Duan W H and Xu Y 2019 *Sci. Adv.* **5** eaaw5685
[22] Otrokov M M, Menshchikova T V, Rusinov I P, Vergniory M G, Kuznetsov V M and Chulkov E V 2017 *JETP Lett.* **105** 297
[23] Xu Y F, Song Z D, Wang Z J, Weng H M and Dai X 2019 *Phys. Rev. Lett.* **122** 256402
[24] Deng Y J, Yu Y J, Shi M Z, Wang J, Chen X H and Zhang Y B 2019 arXiv:1904.11468 [cond-mat.mtrl-sci]
[25] Liu C, Wang Y C, Li H, Wu Y, Li Y X, Li J H, He K, Xu Y, Zhang J S and Wang Y Y 2020 *Nat. Mater.* **19** (in press)
[26] Li H, Gao S Y, Duan S F, Xu Y F, Zhu K J, Tian S J, Gao J C, Fan W H, Rao Z C, Huang J R, Li J J, Yan D Y, Liu Z T, Liu W L, Huang Y B, Li Y L, Liu Y, Zhang G B, Zhang P, Kondo T, Shin S, Lei H C, Shi Y G, Zhang W T, Weng H M, Qian T and Ding H 2019 *Phys. Rev. X* **9** 041039
[27] Arguilla M Q, Cultrara N D, Baum Z J, Jiang S, Ross R D and Goldberger J E 2017 *Inorg. Chem. Front.* **4** 378
[28] Gui X, Pletikosic I, Cao H B, Tien H J, Xu X T, Zhong R D, Wang G Q, Chang T R, Jia S, Valla T, Xie W W and Cava R J 2019 *ACS Cent. Sci.* **5** 900
[29] Kawakami N and Okiji A 1986 *J. Phys. Soc. Jpn.* **55** 2114
[30] Rojas D P, Fernandez J R, Espeso J I and Gómez Sal J C 2010 *J. Alloys Compd.* **502** 275
[31] Yamada H and Takada S 1973 *J. Phys. Soc. Jpn.* **34** 51
[32] Hundley M F, Hawley M, Heffner R H, Jia Q X, Neumeier J J, Tesmer J, Thompson J D and Wu X D 1995 *Appl. Phys. Lett.* **67** 860
[33] Emin D and Liu N L H 1983 *Phys. Rev. B* **27** 4788